Glycine receptor complex analysis using immunoprecipitation-blue native gel electrophoresis-mass spectrometry

Sophie J. F. van der Spek[1], Frank Koopmans[1], Iryna Paliukhovich[1], Sarah L. Ramsden[2], Kirsten Harvey[2], Robert J. Harvey[3,4], August B. Smit[1] and Ka Wan Li[1]

1. Department of Molecular and Cellular Neurobiology, Center for Neurogenomics and Cognitive Research, Amsterdam Neuroscience, Vrije Universiteit, Amsterdam, The Netherlands
2. Department of Pharmacology, UCL School of Pharmacy, London, United Kingdom
3. School of Health and Sport Sciences, University of the Sunshine Coast, Maroochydore DC, Queensland, Australia
4. Sunshine Coast Health Institute, Birtinya, Queensland, Australia

Corresponding author: Ka Wan Li, Department of Molecular and Cellular Neurobiology, Faculty of Science, Vrije Universiteit Amsterdam, De Boelelaan 1085, 1081HV, Amsterdam, The Netherlands. E-mail: k.w.li@vu.nl

Abstract

The pentameric glycine receptor (GlyR), comprising the α1 and β subunits, is a major inhibitory ionotropic receptor in brainstem and spinal cord. GlyRs interact with gephyrin (GPHN), a scaffold protein that anchors the GlyR in the plasma membrane and enables it to form clusters in glycinergic postsynapses. Using an interaction proteomics approach, we provide evidence of the ArfGEFs IQ motif and Sec7 domain 3 (IQSEC3) and IQ motif and Sec7 domain 2 (IQSEC2) as two novel synaptic proteins interacting with GlyR complexes. When the affinity-isolated GlyR complexes were fractionated by blue native gel electrophoresis and characterized by mass spectrometry, GlyR α1β-GPHN appeared as the most abundant complex with a molecular weight of approximately 1 MDa, and GlyR α1β-GPHN-IQSEC3 as a minor protein complex of approximately 1.2 MDa. A third GlyR α1β-GPHN-IQSEC2 complex existed at the lowest amount with a mass similar to the IQSEC3-containing complex. Using yeast two-hybrid we demonstrate that IQSEC3 interacts with the GlyR complex by binding to the GPHN G domain at the N-terminal of the IQSEC3 IQ-like domain. Our data provide direct evidence of the interaction of IQSEC3 with GlyR-GPHN complexes, underscoring a potential role of these ArfGEFs in the function of glycinergic synapses.

Accepted Article

Number of words: 6537

Significance of the study

Affinity purification-based interaction proteomics has been extensively used to reveal the protein constituents of protein complexes. However, it does not allow to determine the organization of these constituents in sub-complexes, which may contain overlapping sets of proteins. In this study, we combined immuno-precipitation and subsequent blue-native gel electrophoresis to resolve sub-complexes according to their masses. We examined the major inhibitory receptor in the peripheral nervous system, the glycine receptor, and demonstrated that the glycine receptor subunits α1 and β together with gephyrin form the main constituents of the GlyR. We further revealed the presence of a minor fraction of the GlyR pool forming a sub-complex with IQSEC3 and, to a lesser extent, with IQSEC2 that migrated to a higher mass on the blue native gel. We confirmed the IQSEC3-gephyrin interaction by yeast two-hybrid analysis.

Introduction

The glycine receptor (GlyR) is an anion-selective ligand-gated ion channel expressed mainly in the brain stem and spinal cord. GlyRs mediate fast inhibitory neurotransmission, and are involved in the regulation of locomotion, respiration and nociceptive processes [1]; e.g., malfunction of the major adult α1β subunit containing GlyR is known to cause startle disease/hyperekplexia [2]. The glycinergic synapse has a relatively simple postsynaptic density at the ultra-structural level [3]. It consists of multiple GlyRs, each composed of a pentamer of α1 and β subunits clustered by the synaptic scaffolding protein gephyrin (GPHN), and is thought to have limited ability for plastic change [3]. Recent interaction proteomics studies on ligand-gated ion channels and membrane receptors, such as GABA$_A$ and glutamate receptors, have revealed the presence of many protein interactors [4-8]. However, the relatively simple composition known of the GlyR complex (GlyR α1β-GPHN) may in part be explained by the low sensitive biochemical methods used in the previous studies, leaving additional interactors undetected. While some potential GlyR interactors have been characterised, including karyopherin 3 and 4 [9], Vacuolar Protein Sorting 35 and Neurobeachin [10], and syndapin I [11], a detailed proteomics analysis of synaptic GlyRs is currently lacking. In this study, we used

immuno-precipitation (IP)-based interaction proteomics to characterize GlyR associated proteins from a brain stem extract. Using the AMPAR interactome as background to identify candidates [4], we identified two ArfGEFs: IQ motif and Sec7 domain 3 (IQSEC3, also known as BRAG3/SynArfGEF) and, to a lesser extent, IQ motif and Sec7 domain 2 (IQSEC2, also known as BRAG1/IQ-ArfGEF) as new GlyR interactors. The IQSEC3 and IQSEC2 interaction with GlyR complexes was validated by using a multi-dimensional IP-Blue native gel electrophoresis (BN)-mass spectrometry (MS) approach. IP-captured protein complexes were size-fractionated by BN and analysed by quantitative proteomics. Correlation profiling of protein migration patterns on the BN gel distinguished several GlyR complexes, of which the main pool consisted of GlyR α1β-GPHN. At the higher molecular weight range IQSEC2 and IQSEC3 were also detected, corresponding to the complexes GlyR α1β-GPHN-IQSEC3 and GlyR α1β-GPHN-IQSEC2. Using yeast two-hybrid, we demonstrated that IQSEC3 interacts with the GlyR complex through the binding of the GPHN G domain with a unique motif (amino acids 160-210) N-terminal of the IQSEC3 IQ-like domain.

Materials and Methods

Immuno-precipitation / SDS-PAGE fractionation. One mouse brainstem was used per IP experiment. Brainstem tissue was homogenized in 1% n- dodecyl β- d- maltoside buffer containing 25 mM HEPES, 150 mM NaCl (pH 7.4) and proteinase inhibitor (Roche), and incubated for 1h at 4ºC. After centrifugation at 20,000 x *g*, 10 µg of antibody was added to the supernatant, and incubated overnight at 4ºC. The antibody was captured by 0.1 mL protein A/G plus agarose beads (Santa Cruz). After washing four times with 0.1% Triton-X buffer containing 25 mM HEPES and 150 mM NaCl (pH 7.4), the beads were mixed with SDS sample buffer and heated to 98°C for 5 min. Proteins were separated on a 10% SDS polyacrylamide gel and stained with Coomassie Blue. Each sample lane was cut into three fractions, each fraction was further cut into small gel pieces and transferred to a 96 well plate (0.45 µm filter; MultiScreen-HV 96 well filter-plate from Millipore). The proteins were destained, digested with trypsin overnight at 37°C and dried in a speedvac as described previously [12].

The IPs of GluA2/3 and GluA4 have also been performed on the hippocampal extract, with one mouse hippocampus per IP experiment, as a control for sensitivity of our IP-MS approach.

A commercially available GlyR α1 antibody (A01636-100; labelled as GlyR α1a), and custom-made antibodies against GlyR α1 (NTTNPPPAPSKSPE; labelled as GlyR α1b), GlyR β *(*NGLGKPQAKNKKPP*)*, GPHN *(*PTPKQIRRPDESKG), GluA2/3 (QNFATYKEGYNVYGIESVKI) and GluA4 (RQSSGLAVIASDLP) obtained from Genscript were used for IP-analysis. The IQSEC3 antibody (sc-324895) was obtained from Santa Cruz.

Immuno-precipitation / peptide elution / BN. The protein input, antibody, and beads used for IPs followed by peptide elution experiments were scaled up 10 times. To elute protein complexes from the antibody, synthetic peptide (0.5 mg/mL) corresponding to the antibody epitope was dissolved in wash buffer, added to the beads after IP and washing, and incubated for 45 min at room temperature. Protein complex elution was performed twice and the supernatant was pooled. Using a 30 kDa cut-off centrifuge filter (Vivaspin 500 from Sartorius), supernatant was concentrated to about 30 µL as input material for BN, while the synthetic peptide was largely removed. The peptide eluted sample was mixed with 5 µL 8× BN loading buffer, 0.5 µL of molecular weight marker and 1 µL 5% G-250 Coomassie blue and loaded on a pre-cast Invitrogen NativePAGE 4-16% Bis-Tris Gel (ThermoFisher). The gel was run at 4°C, 150 V for 1.5h, followed by 250 V for 1h. The gel was fixed overnight, washed 3× in water, and cut with a grid cutter (The Gel Company) into 48 equal sized pieces. Each piece was transferred individually to a well in a 96-well filter plate (0.45 µm filter; MultiScreen-HV 96 well filter-plate from Millipore) for destaining and trypsin digestion.

Trypsin digestion. The gel pieces in the well of a 96-well filter plate were destained with sequential application and centrifugation removal of 50 mM NH_3HCO_3/50% acetonitrile and 100% acetonitrile with incubation times of 20 min and 5 min, respectively, and NH_3HCO_3/50% acetonitrile incubation overnight. After dehydration in 100% acetonitrile, the gel pieces were incubated with MS grade endo lysC/Trypsin (Promega) at 37 ºC overnight. The resulting peptides were extracted with 0.1% TFA in 50% and 80% acetonitrile, 20 min each, dried in the SpeedVac and subjected to MS analysis.

HPLC-ESI MS/MS and data analysis. The TripleTOF 5600+ MS was coupled to an Ultimate 3000 LC system (Dionex, Thermo Scientific).

For IP-BN samples, the MS was run in nano-mode. Peptides were re-dissolved in 7 µL of 2% acetonitrile with 0.1% formic acid, loaded onto a 5 mm Pepmap 100 C18 column, and then fractionated on a 200 mm Alltima C18 homemade column (100 µm i.d., 3 µm particle size) using 0.1% formic acid with a linear gradient of increasing acetonitrile concentration from 5% to 30% in 35 min, to 40% at 37 min and to 90% for 10 min at a flow rate of 500 nL/min. Peptides were electro-sprayed into the MS using an ion spray voltage of 2500 V, ion source gas at 2 p.s.i., curtain gas at 35 p.s.i and an interface heater temperature of 150°C.

For IP samples, the MS was run in micro-mode. Peptides were fractionated on a 200 mm Alltima C18 column (300 µm i.d., 3 µm particle size) at a flow rate of 5 µl/min, with the same gradient as the nano-mode. The eluted peptides were electro-sprayed with a micro-spray needle voltage of 5500 V.

The MS survey scan range was *m/z* 350–1250 acquired for 250 ms. The top 20 precursor ions were selected for 90 ms per MS/MS acquisition, with a threshold of 90 counts. Dynamic exclusion was 10 s. Rolling CID function was activated, with an energy spread of 5 eV. The MS/MS spectra were

searched against the Mouse database (UP000000589_10090) using MaxQuant software [13] (version 1.6.3.4). For IP-BN data, unique high quality peptides were manually curated in Skyline [14] for further analysis.

IQSEC3 IPs were processed with FASP and analysed using a LTQ-Orbitrap [6] (see supplementary material and methods).

The mass spectrometry proteomics data have been deposited to the ProteomeXchange Consortium via the PRIDE partner repository with the dataset identifier PXD01715.

Yeast two-hybrid assays. Yeast two-hybrid assays and *LacZ* freeze fracture assays were carried out as previously described, using the yeast strain Y190 and GAL4 vectors pYTH16 and pACT [15]. GPHN constructs encoded the rat GPHN G domain (amino acids 1-173), C domain (173-323), E domain (323-736) or full-length GPHN (1-736), while those for rat IQSEC3 encoded amino acids 1-649 (N-terminus), 1-1182 (full length) or 50 amino acid overlapping N-terminal fragments (1-50, 40-90, 80-130, 120-170, 160-210, 200-250, 240-290, etc). Control baits for the rat GPHN G domain (1-173) and GlyR β subunit intracellular loop were as previously described [15]. Co-transformed yeast were plated on selective dropout media lacking leucine and tryptophan (Takara) and incubated at 30°C for 3-6 days to allow prototropic colonies to emerge.

Results

In this study we examined the interactome of the major adult GlyR (α1β) subtype by immuno-precipitating the GlyR subunits GlyR α1, β and GPHN and identifying interacting proteins by mass spectrometry. For this we used a commercially available GlyRα1 antibody obtained from Genscript (anti-GlyRα1a) and three custom-made antibodies raised against GlyRα1 (anti-GlyRα1b), GlyRβ and GPHN, which recognised the bait proteins specifically (Supplementary Fig. 1A, see also Supplementary Materials and Methods). In addition, to distinguish the bulk of proteins binding in the IPs from GlyR-specific interactors, two custom-made antibodies raised against the AMPA-receptor subunits GluA2/3 and GluA4 (Supplementary Fig. 1A) were used as background to identify candidates [6, 16].

In the first instance, we examined the effect of different detergents on integrity of the GlyR protein complex. Brain stem proteins were extracted in 1% DDM, NP-40 and Triton X-100, and run on a blue-native gel and stained for GlyRβ. Clear immuno-reactivity for the GlyR was observed around 1 MDa for all three extraction conditions, and a lack of signal around 50 kDa, i.e., the molecular weight of single GlyR subunits. Triton X-100 and NP-40 conditions showed immuno-reactivity around 700 kDa, which may implicate mild breakdown of the protein complex during extraction (Supplementary

Fig.1B). In addition, DDM was previously found as preferred detergent for maintaining the integrity of the AMPA receptor protein complex [4]. We therefore used 1% DDM for subsequent experiments.

To obtain high consistency in our IP-MS/MS experiment, volumes, protein concentrations and amount of antibody used, were kept constant. In addition, four biological replicates for all GlyR/GPHN and AMPAR antibodies were performed in a single batch. The IP samples were run on SDS-PAGE gel, cut into three fractions, trypsin digested and analysed by LC-MS/MS. This classic approach is more labour intensive and time consuming than the recently developed FASP and SP3 methods [6, 17] . However, the advantages are that it allows for quality control of the IP experiments by staining the proteins on the SDS-PAGE gel (Supplementary Fig. 2), while the fractionation and separate LC-MS/MS of each fraction increases the depth of the proteomics analysis. The control GluA IPs in brainstem and hippocampus consistently purified the previously reported AMPA receptor interactors [4, 7], which were not present in the GlyR and GPHN IP sets, indicating the reliability and high sensitivity of the approach (Supplementary Fig. 3). For enrichment analysis, only brainstem GluA-IPs were used to filter out background proteins. Figure 1A shows the iBAQ intensity values of proteins present in >75% of the GlyR/GPHN IP experiments (i.e. > 12 out of the 16 IP experiments) with an iBAQ enrichment of ≥10 fold compared to the GluA2/3 and GluA4 IPs. The complete list of proteins detected in each individual IP of all antibodies used in this analysis is given in supplementary Table 1. Overviews of the IP data per antibody, highlighting the fold change ranking of the interactors are provided in Supplementary figure 4.

The core proteins GlyR α1, GlyR β and GPHN, were recovered from the GlyR α1 and GlyR β IPs, in here GPHN was detected as the most abundant protein. Similar results were obtained from GPHN IPs. GlyR α2 and α3 were detected as well, albeit at a considerable lower amount. Interestingly, we detected two ArfGEFs, IQSEC3 and IQSEC2, which were purified at 10 to 100 fold lower levels, respectively, than the GlyR and GPHN. Two additional potential interactors were present at similar low detection level, NRXN3 and GPC1.

Among the several novel potential GlyR interactors, IQSEC3 is detected at the highest level that is nevertheless about 10 fold lower than GlyR and GPHN. To validate the GlyR-IQSEC3 interaction, we performed reverse IPs on IQSEC3 (Fig. 1B, supplementary Table 2). GPHN was recovered at a 5x lower level than IQSEC3, and GlyR α1 at a 20x lower level. This suggests a primary interaction between IQSEC3 and GPHN, with the GlyR as secondary interaction via GPHN. IQSEC2 was not recovered from the IQSEC3 IPs, suggesting that IQSEC2 and IQSEC3 are contained in distinct complexes.

To discern different protein complexes, we extended the IP approach with mass separation of native protein complexes by blue-native gel electrophoresis followed by their proteomics analysis (IP-BN

Proteomics; Fig. 2A), focussing on the core proteins GlyR α1 and GlyR β. As a protein contained in a complex likely will spread out across multiple BN gel fractions resulting in a lower protein amount in individual BN gel fractions, the IP experiments were scaled-up ten-fold to compensate for the dilution across gel fractions. To reveal the validity of the BN-MS approach, we first tracked unique tryptic peptides derived from a single protein as these should provide the same migration pattern on the BN gel. A representative example is provided by the three tryptic peptides of GlyR α1 on the GlyR β IP-BN (Figure 2B). We observed pronounced intensity differences between the peptides. When the intensities are normalized to 100% at their maximum, their highly correlated migration patterns become apparent (Pearson's correlation ≥ 0.99) (Fig. 2C).

To achieve the most accurate migration profiling of the proteins across the gel, the summed intensities from individually peak-picked peptides in Skyline were plotted (Fig. 2D). Peptides chosen for curation in Skyline included those that are unique for the protein of interest, preferably unmodified and most abundant. Highly correlated migration profiles of GlyR α1, GlyR β and GPHN (Pearson's correlation ≥ 0.99) were observed, implying that they are part of the same complex (Fig. 2E). Of note, four marker proteins were included as reference for molecular weight. The main GlyR-GPHN complex peaked at approximately 1 MDa. In addition, a small fraction of the GlyR subunits were detected in a lower mass range between 480 and 720 kDa without GPHN. IQSEC2 and IQSEC3 were recovered at a ten to hundred-fold lower level than the GlyR and GPHN from IP experiments (Fig. 1). Both proteins were also recovered from the IP-BN experiments. When plotted against the subunits of the GlyR, IQSEC3 has a lower intensity (Fig. 3A) and peaked at the high mass range of the GlyR complex in the BN at approximately 1.2 MDa (Fig. 3B). Thus, the GlyR-GPHN-IQSEC3 protein complex presents as a minor component with a larger MW than the average of the GlyR-GPHN complex (Fig. 3A-B). IQSEC2 showed a similar migration pattern on the BN gel. It was present also at slightly lower MW than IQSEC3 and with substantially lower intensity.

The initial IP-MS analysis (Fig. 1) showed the presence of several additional putative GlyR interactors at low intensities. In the IP-BN proteomics experiments, NRXN3 and GPC1 both migrated at a low MW range of <420 kDa that do not overlap with the detection of the GlyR subunits (Fig. 3 C-D). To conclude, the majority of the GlyR protein complex represents the GlyR receptor and GPHN, and a small population of the GlyR complex contains IQSEC2 or IQSEC3.

To reveal the reproducibility of this approach, we isolated the GlyR complexes using two different anti-GlyR α1 antibodies, and examined their migration pattern on the BN gel (Fig. 3E-H). Similar to the results of the GlyR β IP-BN-MS experiment, GlyR α1-β-GPHN show highly correlated migration profiles and peaked at approximately 1 MDa. IQSEC2 and IQSEC3 again appeared in the higher mass range of the GlyR complex with substantially lower intensities than the GlyR core proteins. Low MW

complexes were also present including one that peaked at approximately 480 kDa that contained GlyR α1 and β subunits but not GPHN.

To unequivocally identify the binding partner of IQSEC3 in the GlyR α1β-GPHN complex, we utilised the GAL4 yeast two-hybrid system. While we were unable to detect interactions between IQSEC3 with GlyR α1 or β subunit baits (data not shown), robust interactions between IQSEC3 and GPHN were detected. To map the reciprocal binding sites for the GPHN-IQSEC3 interactions, we assessed interactions with IQSEC3 and GPHN G, C and E domains, using GPHN G domain trimerisation, and GlyR β-GPHN E domain interactions as positive controls. The GPHN E-domain interacted with GlyR β (Fig. 4A). Interestingly, this analysis revealed that full-length IQSEC3 and the N-terminus of IQSEC3 (amino acids 1-649) interacted with the GPHN G domain, but not the C or E domains (Fig. 4A). Furthermore, we screened 8 overlapping IQSEC3 baits against GPHN G domain to reveal the specific binding site of IQSEC3 to GPHN. A single bait (amino acids 160 and 210 of IQSEC3) yielded strong signal, situated upstream of the regulatory IQ-like domain (at amino acids 316-326, Fig. 4B). Taken together, we validated the IQSEC3-GPHN interaction and located to a core GPHN G domain binding motif on IQSEC3.

Discussion

Our interaction proteomics study suggests that the major adult GlyR α1β subtype contains mainly GlyR α1, GlyR β and GPHN. This organization was initially demonstrated three decades ago by the affinity isolation of the GlyR on an aminostrychnine-agarose column which showed the presence of three main protein bands after separation of the receptor complex on the SDS-PAGE gel [18]. We now provide evidence that the ArfGEF IQSEC3 is an additional partner in GlyR complexes, via an interaction between the IQSEC3 N-terminus and the GPHN G domain. Existence of additional more labile interactors, and interactors shared by the GlyR and AMPAR cannot be excluded.

Immuno-precipitation of a protein using an antibody followed by proteomics analysis is a well-established technique to reveal the individual components of protein complexes [17]. In addition to the quality of the antibody, the ability to filter contaminants is equally critical to the success of the experiment. Often, hundreds of proteins are identified in a single IP, most of them are false positives bound non-specifically to the antibody or beads causing random noise. Furthermore, antibodies may show cross-reactivity, recognizing additional proteins with their specific sites yielding false positives, or target the bait protein at the site of protein-protein interaction giving rise to false negatives. Multiple strategies can be used to reveal false positives, including the use of gene knockout tissue [6, 19], peptide-blocking the antibody specific site using the antigen peptide [16], or including multiple antibodies against other non-related target proteins.

In the present study, we used a comparative analysis of four antibodies against GlyR α1, GlyR β and GPHN, and two antibodies against the excitatory AMPAR. Using the criterion of abundance difference, resulting in a high percentage of true positives for the AMPAR, we were able to select potential GlyR-specific protein interactors. Subsequent BN-PAGE MS/MS revealed the interaction of IQSEC 2 and 3 to GlyR forming sub-complexes with higher masses (>1 MDa).

With our IPs we were able to identify both IQSEC3 and IQSEC2 as part of GlyR complexes, and we confirmed that IQSEC3 is an interactor of the GPHN G domain. The observation that IQSEC3 and IQSEC2 exist in the GlyR IPs at lower amount than GlyR-GPHN, suggests that they are found in sub-complexes of the α1β GlyRs. To improve insight into these GlyR sub-complexes, we used a combination of immunoprecipitation and BN for their separation and identification.

Stable constituents of a protein complex should co-migrate in a biochemical separation medium in which the migration pattern of the complex is defined by the overall physico-chemical properties of the protein constituents. Various native separation methods have been used to fractionate intact protein complexes, which include ion-exchange chromatography, sucrose gradient centrifugation, size exclusion chromatography and BN [20]. The commercially available BN gel enables the reproducible separation of protein complexes that span between 200-1400 kDa. We combined IP with BN to size separate and then characterize the distinct protein sub-complexes of the GlyR. The highest intensities were observed for the three core GlyR proteins. The ~3 times higher mean intensity of GPHN compared to GlyR α1 and GlyR β, and the high apparent molecular weight of the GPHN containing complex(es) is in line with the clustering ability and scaffolding function of GPHN. The two terminal domains of GPHN (G and E) can trimerize and dimerize, respectively, and oligomerize into hexagonal scaffolds. These lattices can be stabilized by GlyR binding and are thought to exist in different packing densities [3]. Pearson correlation of IQSEC3 migration pattern to that of GlyR-GPHN is around 0.4-0.6, which is substantially lower than the ~0.9 among GlyR subunits and GPHN. IQSEC3 co-migrated with a subfraction of the GlyR-GPHN complex at the high mass end of 1.2 MDa. The lower intensity of IQSEC3 may indicate the interaction of this protein to the protein lattice containing multiple copies of GlyR-GPHN.

By using a yeast two-hybrid approach, we validated the IQSEC3-GPHN interaction and identified the binding site in a previously uncharacterized region of IQSEC3 (between amino acids 160 and 210), upstream the IQ-like domain. Interestingly, IQSEC3 was found interacting with the G domain of GPHN, whereas GlyR β-subunit bound to the E domain. This suggests that IQSEC3, GPHN and GlyR can coexist within the same protein complex, in agreement with our previous experiments. IQSEC3 may influence the trimerization of GPHN by interacting with the G domain, leading to the regulation of GPHN clustering and inhibitory synapse formation [21].

Previous studies have also revealed the co-localization of IQSEC3 with GPHN, GABA$_A$Rs and GlyRs at inhibitory synapses in mouse retina [22] and biochemical interactions with GPHN [21, 23]. Labelling with iBioID using Bira-GPHN demonstrated the presence of IQSEC3 in the vicinity of GPHN within GABAergic synapses [24]. Thus, previous studies have indicated evidence that IQSEC3 may be part of inhibitory GABA$_A$R complexes. In the pHluorin/Myc-tagged GABA$_A$R pulldown experiment that identified 149 putative GABA$_A$R interactors, IQSEC3 ranked in the middle of the protein list in terms of peptide count [25]. However, IQSEC3 was not identified in a recent GABA$_A$R γ2-subunit pull down study [5]. Nonetheless, IQSEC3 is clearly involved in the organisation of GABAergic synapses, in particular the correct alignment of the GABAergic pre- and postsynaptic compartments [23]. Curiously, we also identified IQSEC2, a known constituent of excitatory post-synaptic densities [26], in GlyR α1β complexes. While this may appear unusual, IQSEC2 was also recently shown by others to interact with GPHN in an *in vitro* system [21], and was clearly identified in our GlyR and GPHN IPs. Taken together, our findings suggest that both IQSEC2 and IQSEC3 interact with GPHN and may play roles in inhibitory glycinergic synaptic transmission, extending the role of IQSEC2 beyond excitatory synaptic transmission.

Another two putative interactors, the presynaptic NRXN3 and the extracellular matrix component GPC1, were detected at a lower molecular weight than the GlyR in the IP-BN experiment. This includes the possibility that both NRXN3 and GPC1 are false positive interactors. Alternatively, the affinity of NRXN3 and GPC1 to GlyR might be labile causing their dissociation from the GlyR complex during the long process of antibody elution/protein complex concentrating and the BN gel electrophoresis. Future studies using, for example, a crosslinking agent to stabilize the interaction may be used to validate their interaction.

Finally, previous studies have reported several interactors of the GlyR that were not identified in our IPs [9]. For example, karyopherin 3 and 4 were identified as GlyR interacting partners using Y2H and GST-pulldown with the TM3-4 loop of GlyR α3 and GlyR α1, respectively. However, the authors found only minimal colocalization between the GlyR and karyopherins using subsequent confocal immunocytochemistry and suggested there might be no strong static interaction between the proteins *in vivo*. The recovery of these types of interactors may also benefit from stabilization of the interaction prior to the IP-MS procedures in future studies.

Conflict of interest

The authors declare that they have no conflict of interest

Acknowledgements

Figures Legends

A

B

Figure 1

Figure 1. Putative GlyR interactors in brainstem extract. (A) Proteins identified by interaction proteomics that were present in > 75% of the GlyR/GPHN IPs with an iBAQ enrichment of ≥10 folds compared to the mean iBAQ intensity observed in GluA2/3 and GluA4 IPs. (B) Reverse IP with an antibody against IQSEC3 showed the presence of GlyR α1 and GPHN. iBAQ intensity values are shown as a log10 value.
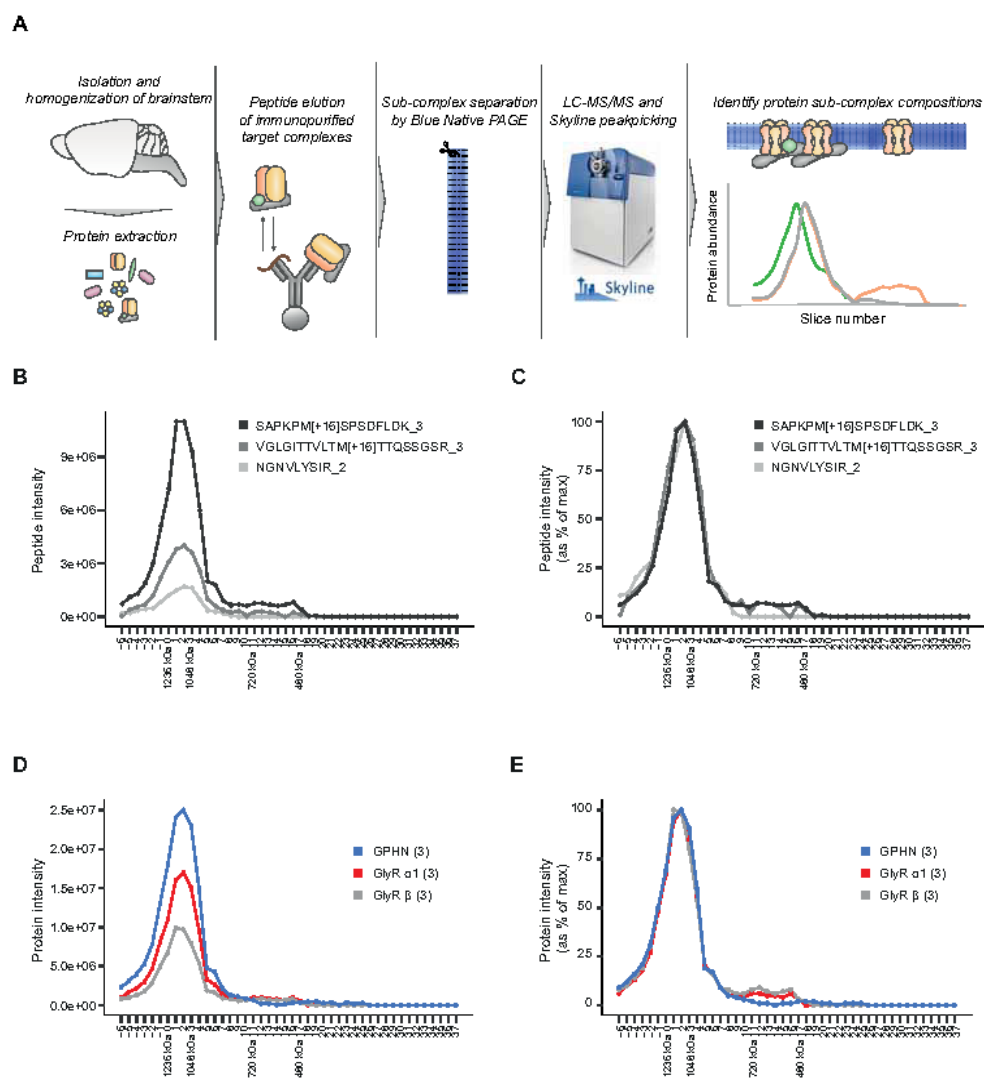
Figure 2

Figure 2. Analysis of the GlyR protein complex by IP-BN proteomics. (A) Workflow of the IP-BN proteomics. Bait protein was immunoprecipitated from tissue extract, and then competed off from the antibody with a synthetic peptide corresponding to the epitope of the antibody. The eluted complexes were size-fractionated by blue native gel electrophoresis. The gel was cut into multiple slices, and analysed by conventional proteomics approach. (B-E) IP-BN mass spectrometry of GlyR β shows identical migration profiles on the BN gel for GlyR α1, GlyR β and GPHN. (B) Three unique GlyR α1 peptides curated in Skyline show similar migration profiles but pronounced differences in intensity values. (C) Normalization of peptide peak intensities to their maximum intensity value reveal the high degree of correlation among the different peptides derived from the same protein (Pearson correlation ≥0.99). (D) GlyR α1, GlyR β and GPHN co-migrate in a molecular weight range peaking at approximately 1 MDa. (E) The normalized data reveals more clearly the high degree of correlation among the different proteins (Pearson correlation ≥0.99) and the presence of a small population of

GlyR α1β complex without GPHN that migrated at a mass between 480-720 kDa. Four marker proteins were included in each IP-BN run as reference for molecular weight, which are depicted on the x-axis. The number of peptides used for peak-picking are shown in brackets.
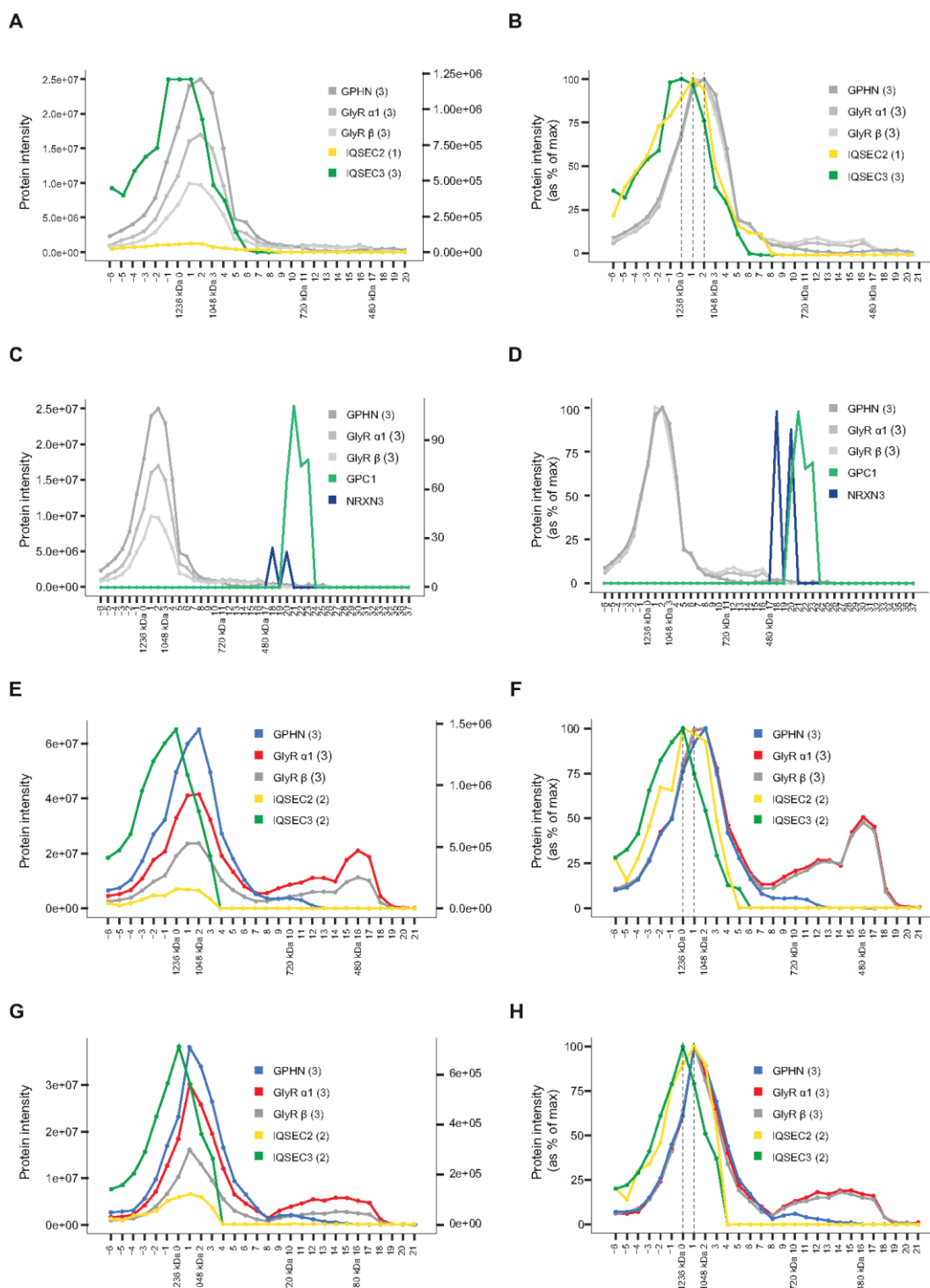

Figure 3

Figure 3. Analysis of GlyR sub-complexes. (A-D) IP-BN mass spectrometry of GlyR β. (A) IQSEC2 and IQSEC3 migrated at the highest molecular weight range of the GlyR. Both IQSEC2 and IQSEC3

show low intensity values (right scale) compared to the GlyR subunits and GPHN (left scale). (B) Normalization of protein peak intensities to their maximum intensity shows that IQSEC2 and IQSEC3 are both present at a high molecular weight (Pearson correlation of IQSEC3 with the GlyR subunits and GPHN is between 0.54-0.56, and of IQSEC2 0.73-0.76). (C) Additional potential GlyR interactors NRXN3 and GPC1 were detected with low intensities (right scale) compared to the GlyR subunits and GPHN (left scale). (D) Normalized data shows a clear detection of NRXN3 and GPC1on the BN gel outside the range of the major GlyR peak (Pearson correlation between -.15 and -0.1), currently excluding these proteins as true interactors. (E-H) Two anti-GlyR α1 IP-BN mass spectrometry (E-F and G-H for two different antibodies, respectively) recapitulate the results obtained for the anti-GlyR β IP-BN. (E and G) The GlyR subunits and GPHN show high intensities (left scale), and IQSEC2 and IQSEC3 were detected with low intensities (right scale) in the GlyR α1 IP-BN experiment. (F and H) Normalized data reveals a tight co-migration of the GlyR subunits and GPHN (Pearson correlation ≥0.87 for F; ≥ 0.97 for H), a small GlyR population without GPHN in the low molecular weight range and IQSEC2 and IQSEC3 at a high molecular weight (F: Pearson correlation IQSEC3 with the GlyR subunits and GPHN is between 0.40-0.44, and of IQSEC2 between 0.84-0.86. H: IQSEC3 with the GlyR subunits and GPHN is between 0.60-0.65, and of IQSEC2 0.91-0.93).

A

B
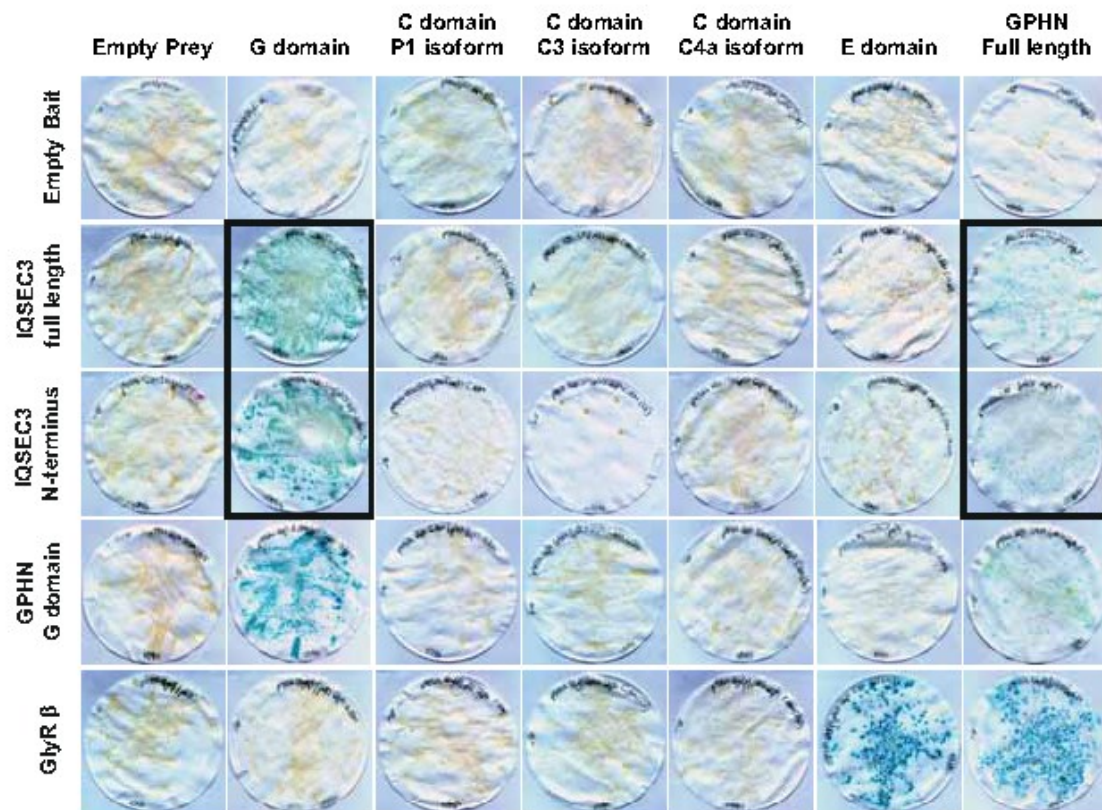
```
MESLLENPVRAVLYLKELTAIVQNQQSLIHTQRERIDELERRLDELSAEN  50
RSLWEHQQLLQAQPPPGLVPPSSAPLPAAPATAPAAAARAQEPLQDQGQR  100
SAAAPHPAPDRPPRQHHGQLLEQPQRGPGSRAHTPQSPHKHLGTQGAVTD  150
```

GPHN

```
KEKERPPSCCAAAGALLQHKSPSALGKGVLSRRPENETVLHQFCCPAADA  200
CSDLASQSDGSCTQAGGGMEDSVVAAAAVAAGRPSAHAPKAQAQELQEEE  250
ERPGAGAASPRAGPQHKASPGRQQPALATALCPHAPAASDYELSLDLKNK  300
QIEMLEHKYGGHLVSRRAACTIQTAFRQYQLSKNFEKIRNSLLESRLPRR  310
```
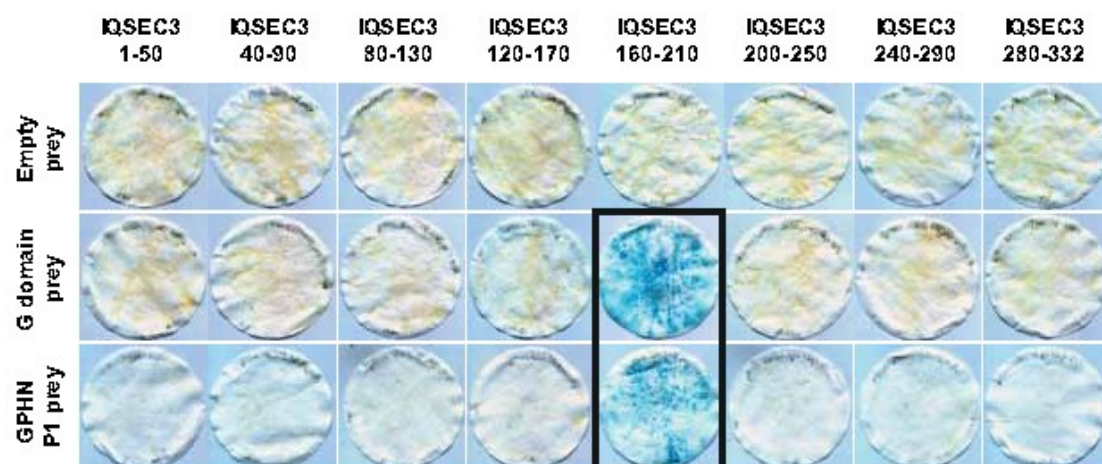
IQ like-domain

Figure 4

Figure 4. Validation of protein-protein interaction by yeast two-hybrid assay. (A) The GAL4BD-IQSEC3 N-terminal fragment (amino acids 1-649) and full-length IQSEC3 interact with GPHN G domain (amino acids 1-173) and full-length GPHN (1-736), but not the GPHN C domain (173-323) or E domain (323-736). G domain:G domain, and GlyR β subunit:E domain interactions utilised as controls, demonstrating that all GPHN preys were correctly expressed. (B)The amino acid sequence of the rat IQSEC3 N-terminus (1-310) depicting the GPHN binding region and IQ-like domain. (c) Assays for overlapping 50-amino acid IQSEC3 baits with GAL4AD (Empty prey), the GPHN G domain, or full-length GPHN, where only fragment IQSEC3 160-210 mediated a robust interaction with the GPHN G domain and full-length GPHN.

References

[1]   J. W. Lynch, Physiol Rev 2004, 84, 1051.
[2]   A. Bode, J. W. Lynch, Mol Brain 2014, 7, 2.
[3]   F. J. Alvarez, Brain Res Bull 2017, 129, 50.
[4]   N. Chen, N. J. Pandya, F. Koopmans, V. Castelo-Szekelv, R. C. van der Schors, A. B. Smit, K. W. Li, J Proteome Res 2014, 13, 5695.
[5]   Y. Ge, Y. Kang, R. M. Cassidy, K. M. Moon, R. Lewis, R. O. L. Wong, L. J. Foster, A. M. Craig, Neuron 2018, 97, 596.
[6]   N. J. Pandya, R. V. Klaassen, R. C. van der Schors, J. A. Slotman, A. Houtsmuller, A. B. Smit, K. W. Li, Proteomics 2016, 16, 2698.
[7]   J. Schwenk, N. Harmel, A. Brechet, G. Zolles, H. Berkefeld, C. S. Muller, W. Bildl, D. Baehrens, B. Huber, A. Kulik, N. Klocker, U. Schulte, B. Fakler, Neuron 2012, 74, 621.
[8]   J. Schwenk, E. Perez-Garci, A. Schneider, A. Kollewe, A. Gauthier-Kemper, T. Fritzius, A. Raveh, M. C. Dinamarca, A. Hanuschkin, W. Bildl, J. Klingauf, M. Gassmann, U. Schulte, B. Bettler, B. Fakler, Nat Neurosci 2016, 19, 233.
[9]   N. Melzer, C. Villmann, K. Becker, K. Harvey, R. J. Harvey, N. Vogel, C. J. Kluck, M. Kneussel, C. M. Becker, J Biol Chem 2010, 285, 3730.
[10]   I. del Pino, I. Paarmann, M. Karas, M. W. Kilimann, H. Betz, Biochem Biophys Res Commun 2011, 412, 435.
[11]   I. Del Pino, D. Koch, R. Schemm, B. Qualmann, H. Betz, I. Paarmann, J Biol Chem 2014, 289, 11396.
[12]   N. Chen, F. Koopmans, A. Gordon, I. Paliukhovich, R. V. Klaassen, R. C. van der Schors, E. Peles, M. Verhage, A. B. Smit, K. W. Li, Biochim Biophys Acta 2015, 1854, 827.
[13]   S. Tyanova, T. Temu, J. Cox, Nat Protoc 2016, 11, 2301.
[14]   L. K. Pino, B. C. Searle, J. G. Bollinger, B. Nunn, B. MacLean, M. J. MacCoss, Mass Spectrom Rev 2017.
[15]   K. Harvey, I. C. Duguid, M. J. Alldred, S. E. Beatty, H. Ward, N. H. Keep, S. E. Lingenfelter, B. R. Pearce, J. Lundgren, M. J. Owen, T. G. Smart, B. Luscher, M. I. Rees, R. J. Harvey, J Neurosci 2004, 24, 5816.
[16]   K. W. Li, N. Chen, P. Klemmer, F. Koopmans, R. Karupothula, A. B. Smit, Proteomics 2012, 12, 2428.
[17]   M. A. Gonzalez-Lozano, F. Koopmans, I. Paliukhovich, A. B. Smit, K. W. Li, Proteomics 2019, e1900027.
[18]   F. Pfeiffer, D. Graham, H. Betz, J Biol Chem 1982, 257, 9389.

[19]   J. von Engelhardt, V. Mack, R. Sprengel, N. Kavenstock, K. W. Li, Y. Stern-Bach, A. B. Smit, P. H. Seeburg, H. Monyer, Science 2010, 327, 1518.

[20]   E. L. Rudashevskaya, A. Sickmann, S. Markoutsa, Expert Rev Proteomics 2016, 1; N. Munawar, G. Olivero, E. Jerman, B. Doyle, G. Streubel, K. Wynne, A. Bracken, G. Cagney, Proteomics 2015, 15, 3603.

[21]   J. W. Um, G. Choii, D. Park, D. Kim, S. Jeon, H. Kang, T. Mori, T. Papadopoulos, T. Yoo, Y. Lee, E. Kim, K. Tabuchi, J. Ko, J Biol Chem 2016, 291, 10119.

[22]   H. Sakagami, O. Katsumata, Y. Hara, H. Tamaki, M. Watanabe, R. J. Harvey, M. Fukaya, J Comp Neurol 2013, 521, 860.

[23]   S. Fruh, S. K. Tyagarajan, B. Campbell, G. Bosshard, J. M. Fritschy, J Neurochem 2018.

[24]   A. Uezu, D. J. Kanak, T. W. Bradshaw, E. J. Soderblom, C. M. Catavero, A. C. Burette, R. J. Weinberg, S. H. Soderling, Science 2016, 353, 1123.

[25]   Y. Nakamura, D. H. Morrow, A. Modgil, D. Huyghe, T. Z. Deeb, M. J. Lumb, P. A. Davies, S. J. Moss, J Biol Chem 2016, 291, 12394.

[26]   J. A. Murphy, O. N. Jensen, R. S. Walikonis, Brain Res 2006, 1120, 35.